

## Coalescence models in nucleon and light ion induced reactions

David H. Boal

*Theoretical Science Institute and Department of Chemistry,  
Simon Fraser University, Burnaby, British Columbia, Canada V5A 1S6*

(Received 23 November 1981)

The coalescence approach to light fragment formation is applied to light ion induced reactions at intermediate energies. These reactions show evidence of a transition between the snowball model for fragment formation in noncomposite particle induced reactions, and the traditional coalescence model of heavy ion reactions. Possible experiments which could be done to better test these ideas are suggested.

NUCLEAR REACTIONS Coalescence models, inclusive reactions,  
light fragment production, nucleon and light ion induced reactions.

## I. INTRODUCTION

We<sup>1-3</sup> have previously proposed that energetic light fragment emission ( $4 \leq A_F \leq 9$ , where  $A_F$  is the mass number of the fragment) at large angles in intermediate energy reactions involves a mechanism in which the projectile strikes a nucleon in the nucleus, and this struck nucleon then undergoes multiple scattering, picking up other nucleons to form the observed fragment. This model, which we called the snowball model,<sup>2,3</sup> was based on the coalescence approach<sup>4,5</sup> and was applied only to noncomposite projectiles, namely electrons and protons.

Another model which involves the coalescence approach is one applied to heavy ion reactions<sup>6-10</sup> in which there are multiple scatterings of the projectile to produce a thermally equilibrated state from which the fragment is ejected. We have argued that such a mechanism cannot be the dominant one for nucleon and electron induced fragmentation since:

(i) The ratio of electron<sup>11</sup> to proton<sup>12</sup> induced alpha emission is roughly the electromagnetic fine structure constant squared. If one assumes that both reactions have a common mechanism, then only one scattering of the projectile can be involved.

(ii) A rapidity analysis of the cross sections of both of these reactions<sup>2,13</sup> shows that the momentum of the hot alpha source would have to be on the order of five times the projectile's momentum, if the target nucleus as a whole is to be the source.

Of course, the snowball and thermal models are meant to be approximations to the many pathways that lead to fragment formation, all of which are

present to some extent in each different projectile-target-fragment combination. It is the purpose of this paper to show that the transition region from snowball dominance to the traditional coalescence model of heavy ion physics, which we will call the final state interaction model (FSI) hereafter, occurs around projectiles of mass number four, depending on the fragment chosen. The following section of this paper will review nucleon induced reactions and show the relative importance of the snowball process compared to the FSI model. Section III will deal with deuteron and alpha particle induced reactions, and show evidence of a transition region. The projectile energy dependence of these reactions will be examined in Sec. IV as a means of probing the reaction mechanism. The conclusions will be summarized in Sec. V, and some experiments which would provide further tests of these ideas will be described. Throughout the paper, our discussion will be confined to that part of the inclusive spectra in which energetic ejectiles (with energies above the low energy evaporation region but not near the kinematic limits) are emitted at large angles to the beam direction. All of the calculations will be done for ejectiles observed at  $90^\circ$ , which we presume is an angle appropriate for the sampling of the "average" reaction mechanism.

## II. NUCLEON INDUCED REACTIONS

We begin our discussion of nucleon induced reactions with the  $(N,p)$  reaction. Many models have been proposed<sup>14-28</sup> to explain the production of energetic ejectiles, ranging from the direct knockout

of a high momentum off-mass-shell nucleon to emission from a hot thermally equilibrated source produced by many nucleon-nucleon collisions. While most models can fit the exponentially falling (as a function of ejectile energy) double differential cross section, only recently has experimental evidence begun to accumulate against a statistical mechanism as being the dominant contribution at the energies under consideration here. One impor-

tant piece of evidence is the ratio of the  $(p,n)$  to  $(p,p')$  cross sections measured at 100 MeV proton energy.<sup>29</sup> A statistical model would predict that above the evaporation region the ratio should be about equal to the neutron to proton ratio of the target, whereas the ratio of cross sections is observed to be roughly half this prediction. In a single scattering model with a coherently recoiling residual system the ratio of cross section is

$$\frac{d^3\sigma(p,n)/d^3q}{d^3\sigma(p,p')/d^3q} = \frac{\int (E_f E_k)^{-1} n(k) N |T_{pn}|^2 d^3p_f \delta(E_p + M_{j+1} - E_f - E_q - E_k)}{\int (E_f E_k)^{-1} n(k) [Z |T_{pp}|^2 + N |T_{pn}|^2] d^3p_f \delta(E_p + M_{j+1} - E_f - E_q - E_k)}, \quad (1)$$

where the kinematic labels are defined in Fig. 1. Here the vertex function  $n(k)$  in plane wave impulse approximation (PWIA) language is the probability of finding a proton (or neutron) of momentum  $-\vec{k}$  in the nucleus and is normalized to unity. The transition matrix element for  $p+n$  scattering in the numerator and denominator are evaluated at different momentum transfer: In the  $(p,p')$  reaction the incident proton charge exchanges with the neutron at small  $u$  ( $u$  being a member of the usual Mandelstam set of variables  $s$ ,  $t$ , and  $u$ ), while in the  $(p,n)$  reaction the proton is scattered forward at small  $t$ , the same value as in the  $p+p$  scattering term. Approximate evaluation of these integrals<sup>29</sup> gives the required factor of about  $\frac{1}{2}$  at 100 MeV. Expanding the treatment of the residual system to include a sum over a variety of recoiling states as suggested in Ref. 16 would not significantly change this result. The  $(p,n)$  and  $(n,p)$  reactions will be discussed further in the following section; the main

point which we wish to make here is that there seems to be evidence that there are only a few scatterings of the projectile and ejectile in nucleon induced nucleon emission. This is not to say that a projectile can produce only one high energy ejectile. Certainly it may scatter several times in a large nucleus, but there is probably only one interaction between an observed ejectile and the projectile.

The snowball model for nucleon induced fragment emission involves an initial interaction to produce a high energy nucleon, as in the direct knockout model, followed by multiple scattering of the struck nucleon to form the observed fragment. This is shown as diagram I in Fig. 2. For calculational simplicity, we will assume that the  $(p,p')$  differential cross section is the same as  $(p,n)$  and simply calculate the cross section for emission of a fragment with  $A_F$  nucleons. Thus, geometrical, combinatoric, and Pauli blocking factors, as well as spin averaging, will be omitted, and the reader is referred to Refs. 3 and 10 for a discussion of their inclusion. We justify omission of these factors on the grounds that we will be concerned with ratios of cross sections throughout most of this paper, and these extra factors will, by and large, cancel out.

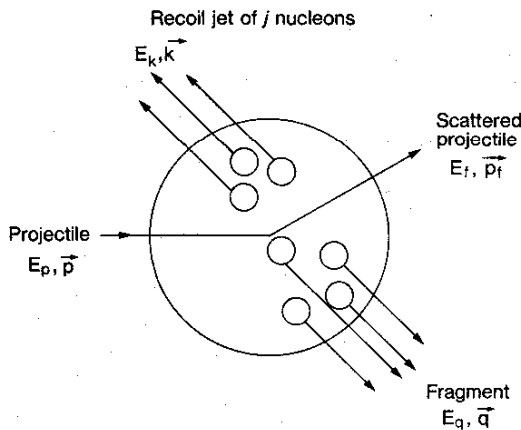


FIG. 1. Kinematic labels for direct knockout of an ejectile (which may be a nucleon) with a coherently recoiling residual system of  $j$  nucleons.

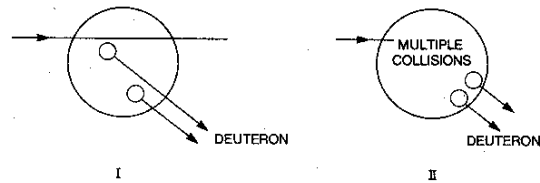


FIG. 2. Two possible contributions to deuteron production. Diagram I represents the snowball model in which a high energy nucleon "picks up" another nucleon to form a deuteron. Diagram II represents the final state interaction model in which two nucleons emitted from the projectile-nucleus interaction region coalesce to form the fragment.

Then, the snowball prediction for the differential cross section is

$$\frac{d^2\sigma}{dE d\Omega}(p,F) = \frac{d^2\sigma}{dE d\Omega}(p,N) \times \sum_i P_i \binom{i}{A_F-1} \mathcal{P}^{A_F-1} (1-\mathcal{P})^{i-A_F+1}. \quad (2)$$

The cross section on the right hand side (rhs) is for a nucleon emitted at the same energy and angle as the observed fragment and arises from the first collision. This struck nucleon, in turn, will undergo several collisions, the probability that it undergoes  $i$  of them being  $P_i$ . At each collision, there is a probability  $\mathcal{P}$  that another nucleon will be scattered into a momentum space volume  $V_s$  around the average momentum per nucleon in the fragment. This volume we take to be

$$V_s = \frac{4}{3} \pi p_s^3 \gamma, \quad (3)$$

where  $\gamma$  is the usual relativistic contraction factor, which we will set equal to unity for the remainder of this paper since the energies considered here are generally nonrelativistic. Because  $\mathcal{P}$  is small, we will approximate this expression by

$$\frac{d^2\sigma}{dE d\Omega}(p,F) = \frac{d^2\sigma}{dE d\Omega}(p,N) \mathcal{P}^{A_F-1} \sum_i P_i \binom{i}{A_F-1}. \quad (4)$$

It is difficult to get an accurate estimate of what the  $P_i$  distribution should be, but a crude approximation would be to have  $P_i$  roughly constant for  $0 \leq i \leq 4$ , for example, and dropping rapidly thereafter. Sample calculations then show that the sum over the product of  $P_i$  and the binomial coefficient is of the order unity for light fragments. In particular, for  $A_F=2$  this sum has a value of between 1 and 2 for several simple distributions chosen. Hence, we will set the sum equal to unity and work with the equation

$$\frac{d^2\sigma}{dE d\Omega}(p,F) = \frac{d^2\sigma}{dE d\Omega}(p,N) \mathcal{P}^{A_F-1}, \quad (5)$$

which will underestimate the fragment cross section in the snowball model for a given  $p_s$ , or equivalently, slightly overestimate the value of  $p_s$  obtained in fits to fragment production data.

Turning now to a value for  $\mathcal{P}$ , the probability that a nucleon will be scattered into  $V_s$  per projectile-nucleus encounter is given by

$$\frac{1}{\bar{M}} \frac{1}{\sigma_R} \frac{d^3\sigma(p,N)}{d^3q} V_s, \quad (6)$$

where  $\bar{M}$  is the mean nucleon multiplicity,  $\sigma_R$  is the reaction cross section, and  $d^3\sigma/d^3q$  is assumed to be sufficiently constant that we have replaced the integral of it over the phase space volume by its product with that volume. The incident energies of interest for the cross sections in Eq. (6) are those of the observed fragments, namely  $100 \pm 50$  MeV. Data<sup>12</sup> at 90–100 MeV incident energy show that, for a target of mass  $A_T$  around 60,  $\sigma_R/A_T$  is about 13 mb/u, while  $A_T^{-1} d^2\sigma(p,p')/dE d\Omega$  is roughly constant at forward angles and has a value of about  $60 \mu\text{b}/\text{MeV sr u}$ . At higher incident energies (or wider ejectile angles)  $d^2\sigma/dE d\Omega$  decreases slowly with ejectile energy, a point with which we will be concerned later in the discussion of  $\alpha$ -induced reactions. The mean nucleon multiplicity is about 3 at these energies, the same as what one would expect for the average number of collisions per projectile-nucleus encounter assuming straight line trajectories and averaging over the impact parameter. Hence, it will be assumed that there is one nucleon emitted per collision in the nucleus, and Eq. (6) is the correct probability for insertion into (5).

The other coalescence approach we will use is that developed in heavy ion physics, which we will call the final state interaction model here, and is shown<sup>30</sup> as diagram II in Fig. 2. In this model, no attention is paid to the details of the projectile-fragment interaction, rather it is assumed that any nucleons emitted with less than a given relative momentum will coalesce. This lack of a constraint on the distance apart that the nucleons can be, yet still form a fragment, probably leads to an overestimate of the cross section for a given  $V_s$ . The form of the expression for the cross section is similar to the snowball expression

$$\frac{d^3\sigma}{d^3p_N}(p,F) = \frac{d^3\sigma}{d^3p_N}(p,N) \frac{1}{A_F!} \left[ \frac{1}{\sigma_R} \frac{d^3\sigma}{d^3p_N} V \right]^{A_F-1}, \quad (7)$$

except that all of the quantities in the expression are evaluated at the same momentum per nucleon  $p_N$ . Again  $\mathcal{P}$  has been assumed to be small. It is also assumed that  $\bar{M} > A_F$ , which is valid for heavy ion collisions or light fragment emission in high energy proton induced reactions. Hence the sum over the multiplicity distribution has been replaced by a delta function at its average value, and, in turn, the  $\bar{M}$  which appears in the binomial coefficient cancels with the  $\bar{M}$  appearing in  $\mathcal{P}$ . The ratio of Eq. (5) to

Eq. (7) can be evaluated using existing data to see what the relative importance of each model is. Shown in Fig. 3 is a calculation of this ratio for the  $A_F=2$  differential cross section at  $90^\circ$  for a 500 MeV incident proton. This proton energy was chosen because of the availability of compatible  $(p,p')$  data<sup>12,31</sup> and reaction cross section data<sup>32</sup> for the energies of interest. A slightly less reliable calculation (because of the lack of data from a medium mass target) has also been made for a 1 GeV incident proton.<sup>33</sup> Both calculations underestimate the falloff with fragment energy which would arise if the integral over phase space in  $\mathcal{P}$  in the snowball model were evaluated more accurately. The fall-off could be in the 30% range over the energy range of the figure. One can see that the snowball contribution is significantly larger than the FSI contribution, although it becomes less so as the ejectile energy increases.

### III. LIGHT ION INDUCED REACTIONS

From the analysis presented above, it would appear that the snowball mechanism is important for light fragment formation in nucleon induced reactions at fragment energies in the 30–150 MeV range. We will now turn our attention to light ion induced reactions to see if there is evidence for a transition to the FSI coalescence model used in heavy ion physics.

One would not expect to find evidence for such a transition in deuteron induced reactions. The deu-

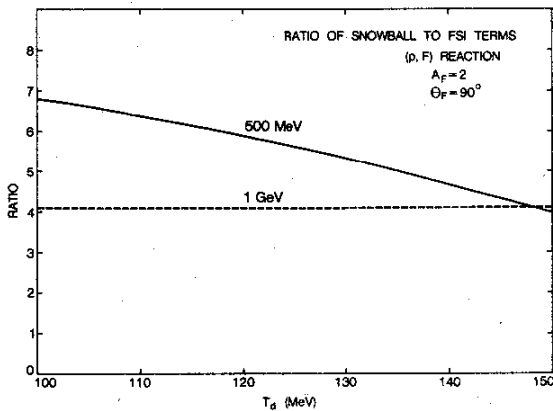


FIG. 3. Ratio of snowball to FSI contributions to two nucleon fragment production from proton bombardment at 500 MeV (solid curve) and 1.04 GeV (dashed curve).

teron is such a loosely bound system that the nucleons probably act independent of one another. Indeed, in a comparison of  $(d,F)$  to  $(p,F)$  differential cross sections, Zebelman *et al.*<sup>34</sup> found that this ratio was a constant as a function of energy (for fragments emitted at  $90^\circ$ ) for  $F=^4\text{He}$ ,  $^7\text{Li}$ ,  $^7\text{Be}$ ,  $^9\text{Be}$ , and  $^{10}\text{Be}$ . The value of the ratio was found to be about 1.5 in a comparison of 2.1 GeV/u deuterons with 4.9 GeV protons. On the basis of  $(p,p')$  data or the estimated energy dependence of the total cross section,<sup>13</sup> this number should be multiplied by a correction factor of 1.3 to 2 to allow comparison of these ratios at the same kinetic energy per incident nucleon. For example, in Fig. 6, the curve drawn through the data points for the  $(p,p')$  reaction on heavy targets ( $T_p=100$  MeV,  $\theta_p \simeq 160^\circ$ ) shows an increase of 1.65 between 2.1 and 4.9 GeV incident proton energy. This would give a value for the  $(d,F)/(p,F)$  ratio of about 2.5, with considerable error. This is roughly what one would expect if the deuteron behaved as two independent nucleons. The exact value which one would expect would depend on the  $(n,F)/(p,F)$  ratio, which may not be unity for a neutron-rich target like uranium.

For the  $(\alpha,p)$  reaction, the direct knockout model would suggest that the differential cross section should obey

$$(\alpha,p)/(p,p')=2[1+(n,p)/(p,p')], \quad (8)$$

independent of energy and angle, if the projectile nucleons are acting independently.

The  $(n,p)$  cross section can be calculated in analogy to Eq. (1). Data<sup>35–37</sup> are available on this ratio for comparison at 1 GeV/u incident energy. The charge exchange ( $u \simeq 0$ ) and elastic ( $t \simeq 0$ ) parts of  $|T_{pn}|^2$  have roughly the same functional form as the  $pp$  elastic amplitude

$$\begin{aligned} |T_{pp}(\text{small } t)|^2 &\equiv 64\pi sp_{c.m.}^2(d\sigma_{pp}/dt) \\ &= 64\pi sp_{c.m.}^2 \times 148 \exp(6.3t), \end{aligned} \quad (9)$$

$$\begin{aligned} |T_{pn}(\text{small } t)|^2 &\equiv 64\pi sp_{c.m.}^2(d\sigma_{pn}/dt) \\ &= 64\pi sp_{c.m.}^2 \times 89 \exp(4.9t), \end{aligned} \quad (10)$$

$$\begin{aligned} |T_{pn}(\text{small } u)|^2 &\equiv 64\pi sp_{c.m.}^2(d\sigma_{pn}/du) \\ &= 64\pi sp_{c.m.}^2 \times 16 \exp(5.7u), \end{aligned} \quad (11)$$

where  $|T|^2$  has units of  $\text{mb}/\text{GeV}^2$  and  $t$  is in units of  $\text{GeV}^2$ . The normalization convention used here

(and throughout) to connect  $|T|^2$  to the differential cross section is the conventional one for the scattering of spin = 0 objects. All of the fits were done at about 1 GeV incident nucleon kinetic energy. The parameters in the exponentials are within about one standard deviation of a value of  $5.5 \text{ GeV}^{-2}$ .

A small peak in the charge exchange reaction between  $0 \leq u \leq -0.05 \text{ GeV}^2$  was omitted in the fit used. Its inclusion would raise the charge exchange contribution by perhaps 15%. However, given the errors caused by comparing these cross sections at different incident energies, the error introduced into the  $(n,p)/(p,p')$  ratio by neglecting this peak is not significant. Because the functional form of the integrands in Eq. (1) are very similar, the rhs can be approximated by the ratio of the intercepts of  $d\sigma/dt$  and  $d\sigma/du$  appropriately weighted. Thus

$$(p,n)/(p,p') = \left[ 1.66 \frac{Z}{N} + 0.18 \right]^{-1}. \quad (12)$$

Similarly,

$$(n,p)/(p,p') = \left[ 1.66 + 0.18 \frac{N}{Z} \right]^{-1}. \quad (13)$$

and

$$(n,n')/(p,p') = \left[ \frac{N}{Z} + 0.11 \right] / \left[ 1 + 0.11 \frac{N}{Z} \right]. \quad (14)$$

For a uranium target, the  $(n,p)/(p,p')$  ratio is equal to 0.51, and Eq. (8) yields

$$(\alpha,p)/(p,p') = 3.0. \quad (15)$$

The experimental value for this ratio, determined by taking smooth fits to the data, is also equal to 3, showing only small variations with energy and angle. A typical result is shown in Fig. 4. In this model, the  $(\alpha,p)/(p,p')$  ratio is predicted to have very little target dependence. Ignoring geometrical factors, Eqs. (8) and (13) predict that this ratio will increase only to 3.1 for a target such as aluminum. We predict as well that the ratio will also change only slowly as the energy is lowered. Taking nucleons with about 400 MeV incident energy as an example, a fit to the data<sup>38,39</sup> gives

$$|T_{pp}(\text{small } t)|^2 = 64\pi s p_{c.m.}^2 \times 62.9 \exp(0.46t), \quad (16)$$

$$|T_{pn}(\text{small } t)|^2 = 64\pi s p_{c.m.}^2 \times 62.9 \exp(1.91t), \quad (17)$$

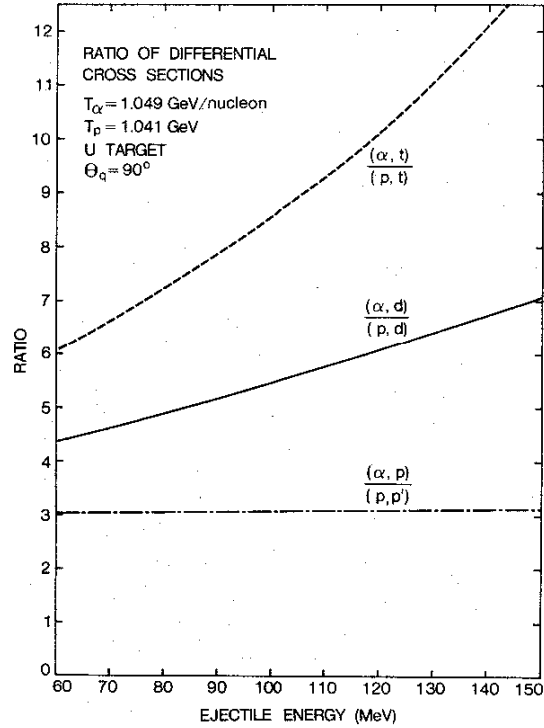


FIG. 4. Experimental ratios of the  $(\alpha, X)/(p, X)$  differential cross sections for  $X = p, d,$  and  $t$ . The data are from Ref. 33 and were measured at 1.04 GeV/u.

$$|T_{pn}(\text{small } u)|^2 = 64\pi s p_{c.m.}^2 \times 114.2 \exp(8.06u). \quad (18)$$

One can see that at this energy, the charge exchange reaction is going to be much more important (again, the small peak at  $u \approx 0$  has been neglected). Because the data do not all have the same functional form (unlike the 1 GeV example), either a detailed numerical integration must be performed, or a more coarse approximation must be made. For our purposes here, the latter will suffice. The integrals involved in Eq. (1) and similar expressions will involve, at this energy, a rapidly falling momentum distribution and slowly varying amplitudes. A very coarse calculation would involve simply removing the amplitudes from the integral and comparing their magnitude. A slightly better approach would be to compare their  $t$  (or  $u$ ) integrals over the range of interest in Eq. (1), usually  $0 \leq -t \leq 0.1$  (similarly for  $u$ ). Adopting this approach, we would predict

$$(p,n)/(p,p') = \left[ 1.09 \frac{Z}{N} + 1.37 \right]^{-1}, \quad (19)$$

$$(n,p)/(p,p') = \left[ 1.09 + 1.37 \frac{N}{Z} \right]^{-1}, \quad (20)$$

$$(n,n')/(p,p') = \left[ \frac{N}{Z} + 1.26 \right] / \left[ 1 + 1.26 \frac{N}{Z} \right]. \quad (21)$$

These ratios will change as the ejectile energy increases and the corresponding range of  $t$  in the integrands changes.

The target dependence of these predictions, as a rough function of  $A_T$ , is shown in Fig. 5. Shown for contrast are the results of Eqs. (12)–(14). These curves have been generated by calculating the ratios for a number of readily available targets, and are not exactly equal to what would be obtained if the minimum of the valley of  $\beta$  stability were followed. Using these ratios, one finds that the  $(\alpha,p)/(p,p')$  ratio declines from about 2.8 for a light target to about 2.6 for a heavy target such as uranium. So, the ejectile energy dependence of this ratio is not very strong, although it may be experimentally detectable.

In summary, the production of protons in alpha induced reactions is consistent with a model in which the projectile nucleons act independently. For production of fragments, this does not appear to be true. Figure 4 also shows the  $(\alpha,d)/(p,d)$  ratio, which clearly has a substantial energy dependence. This behavior poses a problem for models in which the fragment is evaporated from a thermally equilibrated source (aside from the difficulties

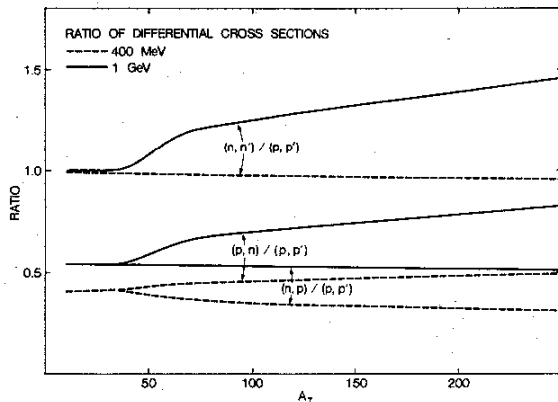


FIG. 5. Estimated target mass number ( $A_T$ ) dependence of various  $(N,N)$  differential cross section ratios in the direct knockout model at 400 MeV (dashed curve) and 1 GeV (solid curve) incident nucleon energy.

raised in Sec. I). In such models, the slope of the differential cross section at a fixed ejectile angle is a measure of the temperature of the source. Nucleon emission in  $p$  and  $\alpha$  induced reactions would indicate that the sources in each of these reactions have the same temperature [since the  $(\alpha,p)/(p,p')$  ratio is constant], while deuteron emission would demand different source temperatures or velocities.

Treating the process of fragment formation as being due solely to the FSI mechanism also produces difficulties. At these bombarding energies, the  $(\alpha,p)$  and  $(p,p')$  differential cross sections are both parametrized at fixed angle as

$$\frac{d^2\sigma}{dE d\Omega}(X,p') = \xi_X(T) \exp(-\beta(T)T_p), \quad (22)$$

where  $X = \alpha, p$  and where  $T$  is the kinetic energy per projectile nucleon. The slope parameter  $\beta(T)$  is the same for  $\alpha$  and  $p$  induced reactions, while the normalization parameter  $\xi_X$  has

$$\xi_\alpha = 3\xi_p. \quad (23)$$

This parametrization shows that there is no ejectile energy dependence in the ratio  $(\alpha,F)/(p,F)$  for the FSI model of Eq. (7). This same kind of reasoning is applicable to a model in which  $\alpha$ -induced fragmentation is due to the snowball model alone.

However, this kind of behavior is what one expects in the transition region between snowball dominance for proton induced reactions, and FSI dominance for heavy ion reactions. A calculation to the accuracy required to test this hypothesis cannot be done at present for lack of input data. However, the general behavior of the transition region can be obtained by considering Eqs. (5) and (7) with the parametrization of Eq. (22). Ignoring constants, the ratio  $R$  of the snowball to FSI contribution to  $\alpha$ -induced deuteron production should be proportional to

$$R \propto \frac{\sigma_{R,\alpha} \xi_\alpha(T) \xi_p(T_q) \exp(-\beta(T)T_q - \beta_p(T_q)T_q/2)}{\sigma_{R,p} \xi_\alpha^2(T) \exp(-\beta(T)T_q)} \\ \propto [\sigma_{R,\alpha} \xi_p(T_q) / \sigma_{R,p} \xi_\alpha(T)] \exp(-\beta_p(T_q)T_q/2), \quad (24)$$

where  $\sigma_{R,i}$  refers to the total reaction cross section in a reaction induced by species  $i$ . We have emphasized that one of the exponents in the numerator is associated with a proton induced reaction by including a subscript  $p$ .

Compared to the ratio of these contributions to proton induced fragment formation, this ratio will be larger because of the extra  $\xi_\alpha$  in the FSI contri-

bution. To some extent, the larger value of  $\xi_\alpha$  compared to  $\xi_p$  [using the incoherence assumption, we have not only  $(\alpha,p)/(p,p')=3$ , but also  $(\alpha,n)/(p,n)\approx 6$ ] will be reduced by the effects of the reaction cross section ratio in Eq. (24). However, the reaction cross section appears to grow much more slowly with the mass number of the projectile than does  $\xi$ , so the FSI contribution will be considerably enhanced, perhaps by a factor of 3. Hence, the two contributions are much more likely to be comparable in magnitude. Further, the snowball contribution should decrease relative to that from the FSI model for increasing  $T_q$  because of the extra  $\beta(T_q)T_q/2$  in the exponent. In the calculation for Fig. 3,  $\beta(T_q\sim 100 \text{ MeV}, \theta_q \text{ forward})$  was set equal to zero as an approximation. In fact, even though it is not nearly as large as  $\beta(\theta_q=90^\circ)$ , nevertheless, it will cause a decrease of perhaps  $\frac{1}{3}$  for a change in  $T_q$  (of the fragment) of 50 MeV at  $\theta_q\approx 20^\circ$ . This is the kind of behavior required by Fig. 4.

For triton emission, the FSI term should dominate over the snowball term, because there will be extra  $\xi_\alpha^2$  in the FSI term. Further, the ratio of the snowball to FSI terms will now go like  $\exp(-2\beta(T_q)T_q/3)$ , so that the snowball contribution will decrease even faster for increasing  $T_q$ . Again, this is the kind of behavior shown in Fig. 4 for triton emission.

In summary, although it is not yet possible to do detailed calculations on the sum of the snowball and FSI contributions, we see that  $\alpha$ -induced fragmentation is inconsistent with the snowball or FSI models alone, but shows a transition between them.

#### IV. PROJECTILE ENERGY DEPENDENCE

A majority of the model analyses of inclusive spectra look only at their variation with ejectile energy and angle, and ignore their variation with projectile energy. This is at least in part attributable to the fact that the detailed energy dependence is often not known experimentally. However, enough data are now available that this energy dependence can be investigated, if only coarsely, and some indication given as to where experimental effort should be put to place the analysis on firmer footing.

Most of the inclusive spectra of the reactions discussed in the previous section vary with projectile energy (at fixed ejectile energy and angle), as shown in Fig. 6. The points are from smooth curves drawn through the data<sup>31,33,40-42</sup> for  $(p,p')$  reactions on heavy targets with the proton being ob-

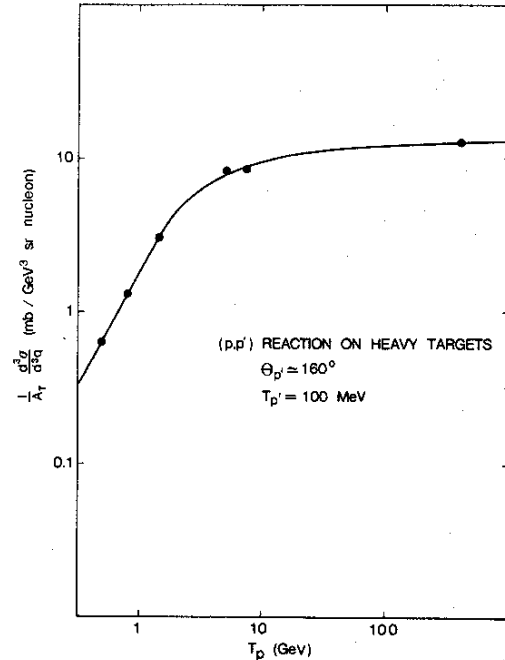


FIG. 6. Behavior of the  $(p,p')$  cross section at fixed ejectile energy and angle as a function of incident proton energy. The targets were Ta and Pb with the proton observed in the  $158^\circ$  to  $162^\circ$  range carrying an energy of 100 MeV. The points are from smooth curves drawn through the data.

served at anywhere from  $158^\circ$  to  $162^\circ$ . One sees that the cross section rises as a power,  $\delta$ , of the incident kinetic energy ( $T^\delta$ ) until about 5 GeV, after which it flattens out to a roughly constant value. The power law dependence of the cross section in the intermediate energy regime is a function of the angle, rising, at  $160^\circ$ , from  $\delta\approx 0.8$  at 50 MeV ejectile energy to 1.5 at 100 MeV ejectile energy. At  $90^\circ$ , this change is less dramatic, although there is a larger error associated with the exponent because the data are considerably more scarce. For an ejectile energy of 50 MeV at  $90^\circ$ , data in the 100–200 MeV incident energy range also appear to obey this power law dependence, and can be used to determine the exponent more accurately. The remainder of this section will be limited to the  $90^\circ$  and 50 MeV kinematic condition for the ejectile angle and energy. Shown in Fig. 7 are data from targets in the  $100 < A_T < 230$  range for the  $(p,p')$ ,  $(p,^4\text{He})$ ,  $(p,^6\text{Li})$ ,  $(\alpha,p)$ , and  $(\alpha,d)$  reactions.<sup>12,13,31,33,43,44</sup> This figure represents the best comparable data which the author could find; "best" meaning similar angles, energies, and targets. Although each line is defined

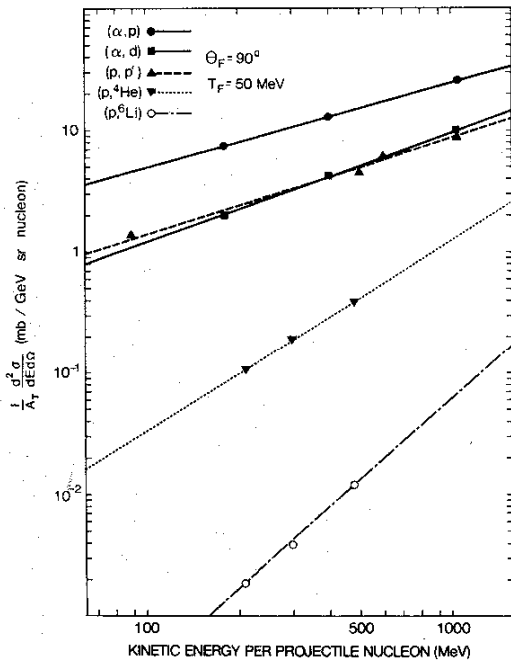


FIG. 7. Behavior of the  $(p, X)$ ,  $X = p', {}^4\text{He}, {}^6\text{Li}$ , and  $(\alpha, X)$ ,  $X = p, d$  cross sections as a function of energy for a 50 MeV ejectile observed at  $90^\circ$ .

by at least three points, it is clear that more data over the 100 MeV–2 GeV region would be most welcome, particularly for the  $(p, d)$  and  $(p, t)$  reactions. The exponents extracted from these curves are listed in Table I.

Comparing first of all the  $(p, p')$  and  $(\alpha, p)$  exponents, one sees that they are very close in value, consistent with the argument presented above that the incident alpha behaves like four independent nucleons as far as nucleon emission is concerned [it will be assumed that the  $(n, p)$  and  $(p, n)$  reactions have the same exponent,  $\delta$ , as does  $(p, p')$ ]. For the  $(p, d)$  and  $(\alpha, d)$  reactions, the two contributions in Fig. 2 for deuteron production will have different

TABLE I. Exponents of the differential cross section per target nucleon as a function of energy per incident nucleon. Ejectile observed at  $90^\circ$ , 50 MeV.

Reaction	References	Exponent ( $\delta$ , in text)
$(p, p')$	12, 31, 33, 43	0.8
$(p, {}^4\text{He})$	13	1.6
$(p, {}^6\text{Li})$	13	2.2
$(\alpha, p)$	33, 44	0.7
$(\alpha, d)$	33, 44	0.9

energy dependence. For fixed ejectile energy and angle, diagram I would have an exponent close to the  $(p, p')$  one at the same ejectile energy and angle, since only one power of the  $(p, p')$  cross section is involved. The other diagram involves the square of the  $(p, p')$  cross section at half the ejectile's energy. For the kinematic conditions here, this latter quantity would involve knowing the  $(p, p')$  cross sections at 25 MeV, at which energy data are not available. Assuming that  $\delta$  is the same at 25 and 50 MeV (this may be a strong assumption and should be checked experimentally), then diagram I would predict  $\delta = 0.8$  for  $(p, d)$  or  $(\alpha, d)$ , while diagram II would predict  $\delta = 1.6$ . We have argued that diagram I should be dominant at these energies, and the value of 0.9 for  $\delta$  is consistent with this.

For  ${}^4\text{He}$  emission, the pure snowball model, shown as diagram I on Fig. 8, would predict an exponent of 0.8. However, mean-free path arguments would indicate that diagrams II and III might be at least as important, since they require a smaller number of collisions along a given nucleon's trajectory. These diagrams would predict an exponent of 1.6, which is in fact the observed value. Again, using the assumption that  $\delta = 0.8$  for the  $(p, p')$  cross section at the appropriate energy per nucleon, the FSI term alone would predict  $\delta = 3.2$  for the  $(p, \alpha)$  reaction. It would be interesting to compare the  $(e, p)$  and  $(e, \alpha)$  exponents in a similar fashion, since there is presumably only one scattering of the projectile in electron induced reactions.

The above analysis, though primitive at present, tends to confirm the conclusions of Secs. II and III. More data on the  $(p, d)$  reaction, the  $(p, p')$  reaction at  $T_p < 50$  MeV, and on all reactions over a wider energy range would be very useful. This kind of analysis should also be applicable to heavy ion reactions, where one would expect the exponents to be

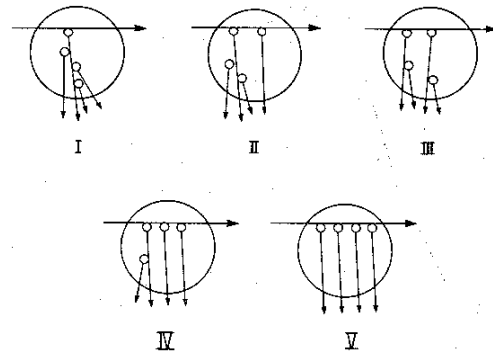


FIG. 8. Several possible contributors to alpha particle formation.



equal to  $A_F$  times the  $(p,p')$  exponent, at the appropriate ejectile energy, if the FSI model is correct.

## V. DISCUSSION AND CONCLUSION

With models that rely so heavily on data input as these do, these ideas will only be really testable when a comparable set of  $(p,X)$  and  $(\alpha,X)$ ,  $X=p, d, t, {}^3\text{He}$  data are obtained at the same incident energy per nucleon and a range of ejectile energies and angles. Information on some of the corresponding  $(n,X)$  reactions would also be useful to check the way in which the neutrons in the alpha have been handled in this calculation. For example, the target and energy dependence of the  $(n,p)$  and  $(p,n)$  reactions as evidenced in Fig. 5 might be checked.

Another issue left aside is the role of charge exchange of the outgoing nucleons. A measure of this could be a comparison of the  $(p,t)$  and  $(p,{}^3\text{He})$  reactions. Unless charge exchange is important, one would not expect these to be the same for  $N=Z$  targets. The heavier the fragment emitted, the more  $N-N$  collisions must be involved, and hence the greater likelihood of charge exchange. Thus, one would expect the effect observed in the  $(p,n)/(p,p')$  ratio to be weaker in  $(p,t)/(p,{}^3\text{He})$  and weaker still in  $(p,{}^7\text{Li})/(p,{}^7\text{Be})$ .

Lastly, the target and projectile energy dependence of light fragment emission should be examined. Good data on the energy dependence would allow the analysis of the previous section to be done much more reliably. The target dependence could shed light on the effects of the distribution,  $P_i$ , of the number of collisions, which has been neglected here. In a small enough target, for a fragment in the mass 10 region, for example, there will not be a sufficiently large number of collisions along a trajectory in the nucleus to allow fragment formation in the snowball model, or equivalently, a high enough multiplicity to allow it in the FSI model. Knowing the average trajectory length, one would be able to obtain information on the interaction length appropriate to a given fragment.

In summary, we have demonstrated in the above analysis that the snowball-like terms in the expression for fragment formation in nucleon induced re-

actions seem to be the dominant contributors over the fragment energy ranges which have conventionally been measured. This conclusion appears to hold for deuteron induced reactions as well, although the conclusion would be on firmer ground if one could compare  $(d,F)$  and  $(p,F)$  data at the same kinetic energy per incident nucleon. However, even when the projectile is as light as an alpha particle, there is evidence that the fragment nucleons may originate in interactions with several different projectile nucleons. This should be contrasted with the  $(\alpha,p)$  reaction, which is well described by the direct knockout model in which the cross sections for the individual incident nucleons are simply added incoherently. That several projectile nucleons may participate in the formation of a fragment in the  $(\alpha,F)$  reactions, but not the  $(d,F)$  reactions, presumably has its origin in the fact that the deuteron is a loosely bound system compared to the alpha, and that the mean multiplicity is less. The FSI model's importance rises rapidly with mean multiplicity, because the FSI contribution is proportional to the projectile nucleus cross section raised to a large power. As one goes to heavy ions, one would expect the FSI model to become the dominant effect, and the  $(\text{HI},F)$  cross section (where HI is a heavy ion) would be proportional to the  $(\text{HI},p)$  and  $(\text{HI},n)$  cross sections (evaluated at the average momentum per fragment nucleon) raised to the appropriate power. Several years ago, this behavior was shown<sup>45,46</sup> for deuterons produced in  $\text{Ar} + \text{KCl}$  collisions at 800 MeV/u [assuming that the  $(p,p')$  and  $(p,n)$  reactions have the same dependence on the emitted nucleon energy], and hopefully future experiments will allow the testing of this model in heavier fragments.

## ACKNOWLEDGMENTS

This work was supported in part by a grant from the Natural Sciences and Engineering Research Council of Canada. The author would like to thank Dr. G. Westfall (Michigan State University) and Dr. S. T. Thornton (University of Virginia) for providing tabulations of data from Refs. 33, and 43 and 44, respectively.

- <sup>1</sup>D. H. Boal, in Proceedings of the Intermediate Energy Nucleon Chemistry Workshop, Los Alamos Report LA-8835-C, 1981.
- <sup>2</sup>D. H. Boal, R. E. L. Green, R. G. Korteling, and M. Soroushian, Phys. Rev. C **23**, 2788 (1981).
- <sup>3</sup>D. H. Boal and M. Soroushian, Phys. Rev. C **25**, 1003 (1982).
- <sup>4</sup>S. T. Butler and C. A. Pearson, Phys. Rev. **129**, 836 (1963).
- <sup>5</sup>A. Schwarzschild and Č. Zupanič, Phys. Rev. **129**, 854 (1963).
- <sup>6</sup>H. Machner, Phys. Lett. **86B**, 129 (1979).
- <sup>7</sup>H. H. Gutbrod *et al.*, Phys. Rev. Lett. **37**, 667 (1976).
- <sup>8</sup>M. -C. Lemaire, Phys. Lett. **85B**, 38 (1979).
- <sup>9</sup>A. Mekjian, Phys. Lett. **89B**, 177 (1980).
- <sup>10</sup>J. I. Kapusta, Phys. Rev. C **21**, 1301 (1980).
- <sup>11</sup>A. G. Flowers *et al.*, Phys. Rev. Lett. **40**, 709 (1978); **43**, 323 (1979).
- <sup>12</sup>J. R. Wu, C. C. Chang, and H. D. Holmgren, Phys. Rev. C **19**, 698 (1979).
- <sup>13</sup>R. E. L. Green and R. G. Korteling, Phys. Rev. C **18**, 311 (1978); **22**, 1594 (1980).
- <sup>14</sup>R. D. Amado and R. M. Woloshyn, Phys. Rev. Lett. **36**, 1435 (1976).
- <sup>15</sup>S. Frankel, Phys. Rev. Lett. **38**, 1338 (1977).
- <sup>16</sup>D. H. Boal and R. M. Woloshyn, Phys. Rev. C **23**, 1206 (1981).
- <sup>17</sup>H. C. Chiang and J. Hufner, Nucl. Phys. **A352**, 442 (1981).
- <sup>18</sup>H. J. Weber and L. D. Miller, Phys. Rev. C **16**, 726 (1977).
- <sup>19</sup>T. Fujita and J. Hufner, Nucl. Phys. **A314**, 317 (1979).
- <sup>20</sup>C. C. Chang, N. S. Wall, and Z. Fraenkel, Phys. Rev. Lett. **33**, 1493 (1974).
- <sup>21</sup>J. R. Wu and C. C. Chang, Phys. Lett. **60B**, 423 (1976).
- <sup>22</sup>M. Blann, Annu. Rev. Nucl. Sci. **25**, 123 (1975).
- <sup>23</sup>R. Weiner and M. Weström, Phys. Rev. Lett. **34**, 1523 (1975).
- <sup>24</sup>T. Nomura *et al.*, Phys. Rev. Lett. **40**, 694 (1978).
- <sup>25</sup>V. I. Bogatin, O. V. Lozhkin, and Yu. P. Yakovlev, Nucl. Phys. **A326**, 508 (1979).
- <sup>26</sup>G. Mantzouranis, D. Agassi, and H. A. Weidenmüller, Phys. Lett. **57B**, 220 (1975).
- <sup>27</sup>J. M. Akkermans, Phys. Lett. **82B**, 20 (1979).
- <sup>28</sup>J. Knoll, Phys. Rev. C **20**, 773 (1979).
- <sup>29</sup>B. D. Anderson *et al.*, Phys. Rev. Lett. **46**, 226 (1981).
- <sup>30</sup>A similar diagram in which coalescing nucleons are emitted directly from the projectile has been investigated by E. A. Remler. For a review of the techniques involved, see E. A. Remler and A. P. Sathe, Ann. Phys. (N.Y.) **91**, 295 (1975).
- <sup>31</sup>G. Roy *et al.*, Phys. Rev. C **23**, 1671 (1981).
- <sup>32</sup>A complication is given in R. M. DeVries and J. C. Peng, Phys. Rev. Lett. **43**, 1373 (1979).
- <sup>33</sup>A. Sandoval *et al.*, Phys. Rev. C **21**, 1321 (1980); G. Westfall, private communication.
- <sup>34</sup>A. M. Zebelman *et al.*, Phys. Rev. C **11**, 1280 (1975).
- <sup>35</sup>B. A. Ryan *et al.*, Phys. Rev. D **3**, 1 (1971).
- <sup>36</sup>M. L. Perl, J. Cox, M. J. Longo, and M. N. Kreisler, Phys. Rev. D **1**, 1857 (1970).
- <sup>37</sup>P. F. Shepard, T. J. Devlin, R. E. Mischke, and J. Solomon, Princeton-Pennsylvania Accelerator Report No. 10, 1969 (unpublished). See also Particle Data Group, NN and ND Interactions (Above 0.5 GeV/c)—A Compilation, Lawrence Radiation Laboratory, Berkeley, Report UCRL-200000 NN, 1970.
- <sup>38</sup>S. K. Kao, H. Horstman, and G. W. Hinman, Phys. Rev. **119**, 381 (1960).
- <sup>39</sup>A. J. Hartzler, R. T. Siegel, and W. Opitz, Phys. Rev. **95**, 591 (1954).
- <sup>40</sup>N. A. Burgov *et al.*, Yad. Fiz. **30**, 720 (1979) [Sov. J. Nucl. Phys. **30**, 371 (1979)].
- <sup>41</sup>S. Frankel *et al.*, Phys. Rev. C **18**, 1375 (1978).
- <sup>42</sup>Y. D. Bayukov *et al.*, Phys. Rev. C **20**, 764 (1979).
- <sup>43</sup>K. R. Cordell *et al.*, Nucl. Phys. **A352**, 485 (1981).
- <sup>44</sup>R. R. Doering *et al.*, Phys. Rev. Lett. **40**, 1433 (1978); S. T. Thornton *et al.*, Phys. Rev. C **19**, 913 (1979).
- <sup>45</sup>S. Nagamiya *et al.*, Phys. Lett. **81B**, 147 (1979).
- <sup>46</sup>M. -C. Lemaire *et al.*, Phys. Lett. **85B**, 38 (1979).